



# Kinetics and thermodynamics of $\beta$ -carotene and chlorophyll adsorption onto acid-activated bentonite from Xinjiang in xylene solution

Zhansheng Wu<sup>a,b</sup>, Chun Li<sup>a,b,\*</sup>

<sup>a</sup> School of Life Science and Technology, Beijing Institute of Technology, Beijing 100081, PR China

<sup>b</sup> School of Chemistry and Chemical Engineering, Shihezi University, Shihezi, Xinjiang 832003, PR China

## ARTICLE INFO

### Article history:

Received 13 January 2009

Received in revised form 13 May 2009

Accepted 10 June 2009

Available online 18 June 2009

### Keywords:

Acid-activated bentonite

$\beta$ -Carotene

Chlorophyll

Xylene solution

Adsorption

## ABSTRACT

The kinetics and thermodynamics of  $\beta$ -carotene and chlorophyll adsorption from xylene solution onto acid-activated bentonite (AAB) within the temperature range 65–95 °C were investigated. Adsorption of  $\beta$ -carotene was described well with the Langmuir isotherm, whereas chlorophyll adsorption was determined well with the Freundlich isotherm, and the experimental data on chlorophyll adsorption were also fitted by the Langmuir isotherm to a certain extent, as reflected by correlation coefficients ( $R^2$ ) over 0.9865. In addition, the adsorption of  $\beta$ -carotene and chlorophyll onto AAB are favorable. The pseudo-second-order model was found to explain the kinetics of adsorption of both pigments more effectively. Increase of temperature enhanced the adsorption rate and equilibrium adsorption capacity of  $\beta$ -carotene and chlorophyll on AAB. The activation energy for the sorption of  $\beta$ -carotene and chlorophyll on AAB was 19.808 kJ/mol and 16.475 kJ/mol, respectively. The thermodynamic parameters  $\Delta H^\theta$ ,  $\Delta S^\theta$  and  $\Delta G^\theta$ , computed from  $K_F$  of the adsorption isotherm constant, were 21.766 kJ/mol, 92.244 J/K mol and  $-9.554$  kJ/mol respectively for the adsorption of  $\beta$ -carotene on AAB at 65 °C, and for adsorption of chlorophyll on AAB at 65 °C were 31.051 kJ/mol, 93.549 J/K mol and  $-0.729$  kJ/mol, respectively. The adsorption of  $\beta$ -carotene and chlorophyll in xylene solution on AAB was a spontaneous and endothermic process with increasing in the randomness at the solid–solution interface.

© 2009 Elsevier B.V. All rights reserved.

## 1. Introduction

Vegetable oils contain numerous pigments, mainly including chlorophyll,  $\beta$ -carotene, xanthophylls and their derivatives, which are removed to give the oil a color that is acceptable to the consumer [1]. Activated clays, activated carbon and silica-based products are adsorbents commonly used in the edible oil decolorization process. Bentonite is highly valued for its sorption properties, which stem from its high specific surface area, swelling capacity and cation exchange capacity (CEC). Some of these properties are related to the crystal isomorphous substitution [2,3]. In addition, the specific surface area, porosity and acid sites are improved with mineral acid activation to yield acid-activated bentonite (AAB) [4]. AAB is widely used in various applications such as catalysts, catalyst supports and a component of carbonless copying papers [5]. Moreover, AAB is the most popular adsorbent for purification, decolorization and stabilization of edible oils as compared to the activated carbon and silica-based products as it is less expensive than activated carbon [6–10]. Also, it removes undesirable compounds such as

$\beta$ -carotene, chlorophyll and other color substances, and reduces traces of  $\text{Cu}^{2+}$  and  $\text{Fe}^{3+}$ , phospholipids, soap and some undesirable oxidation products during bleaching [11].

Most of the previous studies were focused on the removal of  $\beta$ -carotene and chlorophyll from various types of oils by AAB [6–10,12]. Only a few attempts were made to describe the adsorption of  $\beta$ -carotene on acid-activated montmorillonite at low temperature (20–40 °C), using acetone or benzene as solvents [13,14], while for chlorophyll, using hexane or acetone were used as solvents [15–17], due to their high volatility of the solvents. Such temperatures are low as compared to those employed during oil bleaching [6].

Studies on the optimum conditions of preparing AAB from the bentonite of Xinjiang in China used for cotton oil bleaching were carried out recently [18]. The bleaching performance of the AAB was good and the application prospect of the product is wide [19]. In addition, adsorption isotherms and knowledge of kinetics and thermodynamic parameters are the main requirements considered for the design of adsorption experiments. In the present study, the experimental data of adsorption of  $\beta$ -carotene and chlorophyll from xylene solution by AAB were fitted by Langmuir and Freundlich equations. The pseudo-first-order and pseudo-second-order models were applied to determine the best fitting of experimental data. Furthermore, the kinetics and thermodynamic parameters for the

\* Corresponding author at: School of Life Science and Technology, Beijing Institute of Technology, Beijing 100081, PR China. Tel.: +86 10 68913171; fax: +86 10 68915956.  
E-mail address: [lichun@bit.edu.cn](mailto:lichun@bit.edu.cn) (C. Li).

### Nomenclature

$C_0$	initial pigment concentration (mg/L)
$C_t$	residual pigment concentration at any time (mg/L)
$C_e$	residual pigment concentration at equilibrium (mg/L)
$Q_t$	adsorbed pigment quantity per gram of adsorbent at any time (mg/g)
$Q_e$	adsorbed pigment quantity per gram of adsorbent at equilibrium (mg/g)
$q_m$	maximum amount of pigment per unit weight of AAB on the surface (mg/g)
$q_{exp}$	adsorbed pigment quantity per gram of adsorbent at equilibrium with experimental values (mg/g)
$k_1$	pseudo-first-order sorption model rate constant ( $\text{min}^{-1}$ )
$k_2$	pseudo-second-order sorption model rate constant (g/mg min)
$K_L$	Langmuir isotherm constant (L/mg)
$K_F$	constant of Freundlich isotherm
$n$	Freundlich adsorption constant
$E_a$	activation energy (kJ/mol)
$\Delta G^\theta$	Gibbs free energy change (kJ/mol)
$\Delta H^\theta$	enthalpy change of adsorption (kJ/mol)
$\Delta S^\theta$	entropy change of adsorption (J/K mol)
$R$	universal gas constant (8.314 J/mol K)
$R^2$	regression correlation coefficient
$T$	temperature (K, °C)

adsorption of the pigments on AAB from xylene solution were calculated to study the adsorption behavior at various temperatures.

## 2. Materials and methods

### 2.1. Materials

The raw bentonite from the deposit of Xiazijie was donated by Xinjiang Xiazijie Bentonite Co. (China). Our previous studies indicated that the sample consisted of predominantly montmorillonite, substantial amounts of quartz and feldspar impurities, in addition to minor amounts of illite and kaolinite [18]. Anhydrous xylene of analytical grade used was obtained from Xi'an Chemicals (China).  $\beta$ -Carotene of HPLC grade (>98%), purchased from Sigma Co. (America), was used to prepare the calibration curve.

### 2.2. Preparation and analyses of AAB

AAB was prepared from the Xiazijie bentonite by reaction with 25% sulfuric acid under stirring for 4 h, at a bentonite to sulfuric acid solution ratio of 1:2 (by mass) [18]. And chemical compositions of the AAB sample were determined and listed Table 1. After drying, AAB was kept in a desiccator containing silica gel for adsorption experiments.

Bulk density of the AAB was determined according to [20]. Particle size analysis was carried out using standard sieves. The surface area, pore diameter and total pore volume of the sample

**Table 1**

Chemical compositions of acid-activated bentonite.

Compositions	Chemical composition						
	SiO <sub>2</sub>	Al <sub>2</sub> O <sub>3</sub>	Fe <sub>2</sub> O <sub>3</sub>	MgO	CaO	Na <sub>2</sub> O	K <sub>2</sub> O
Content (%)	69.21	12.65	3.82	1.08	0.65	0.49	1.70

were measured by adsorption–desorption isotherm of nitrogen at 77.4 K using an automated specific surface area and porosity analyzer NOVA4000 (Quanta-chrome, Ltd. USA). Before measurement the sample was outgassed at 200 °C for 4 h under vacuum. Specific surface area was calculated using Brunauer–Emmitt–Teller (BET) equation. Bulk density, particle size, specific surface area, pore diameter and total pore volume of the sample were obtained and listed in Table 2. The AAB has low bulk density and high specific surface area, average pore diameter and total pore volume (203.3 m<sup>2</sup>/g, 5.869 nm and 0.2983 ml/g, respectively), which could make an important contribution to the adsorption capacity [19].

### 2.3. Preparation and determination of $\beta$ -carotene and chlorophyll stock solution

$\beta$ -Carotene was extracted from dried carrot [21] and chlorophyll (mixture of chlorophyll a and chlorophyll b) was extracted from dried clover [22].  $\beta$ -Carotene and chlorophyll were dissolved in anhydrous xylene.

$\beta$ -Carotene and chlorophyll concentration in xylene supernatant solution was measured before and after adsorption using an UV–vis spectrophotometer (Cintra20, GBC Scientific Equipment Pty Ltd., Australia). The absorbance of  $\beta$ -carotene measured using the UV–vis spectrophotometer at 457 nm can be transformed to the  $\beta$ -carotene concentration using the calibration curve, which was obtained according to the absorbance of different concentration  $\beta$ -carotene solutions measured using the UV–vis spectrophotometer at 457 nm, the equation of calibration curve was obtained as  $C = 0.0101A_{457} - 0.013$ , and  $R^2$  was equal to 0.9994, it was valid in the study. In addition, the absorbance of chlorophyll measured using the UV–vis spectrophotometer at 646 nm and 663 nm can be calculated to chlorophyll concentration according to Arnon formula [23]: chlorophyll concentration (mg/L) =  $[20.2A_{646} + 8.02A_{663}]$ .

### 2.4. Procedure for adsorption

For each experiment, 25 ml of pigment solution ( $\beta$ -carotene or chlorophyll) of known initial concentration were added in a 100 ml conical flask. To establish thermal equilibrium before adsorption, the flask containing solution was kept agitated at 200 rpm for 15 min in a water bath of desired temperature in the dark, and 0.125 g of AAB were added to the solution. After designed time, the samples were centrifuged immediately and the supernatant solution was analyzed to determine quickly the remaining concentration with the UV–vis spectrophotometer.

The results were reported as the units of adsorbed  $\beta$ -carotene and chlorophyll quantity per gram of adsorbent,  $Q_e$  and  $Q_t$  (mg/g), at equilibrium and at any time, respectively; as unadsorbed pigment concentration in solution at equilibrium and at any time  $C_e$  and  $C_t$  (mg/L), respectively;  $Q_e$ , was obtained from Eq. (1)

$$Q_e = \frac{V(C_0 - C_e)}{m} \quad (1)$$

where  $C_0$  is the initial concentration of the pigment,  $V$  is the volume of the solution, and  $m$  is the amount of dry AAB. When  $C_t$  is used instead of  $C_e$  in Eq. (1),  $Q_t$  is obtained.

The initial concentrations of  $\beta$ -carotene and chlorophyll in anhydrous xylene solution for construction of the adsorption isotherm were 377–753 mg/L and 21.5–63.7 mg/L, respectively, for contact time 90 min. In the kinetic experiments the initial concentrations of  $\beta$ -carotene and chlorophyll were 471 ml and 42.6 ml, respectively, and the reaction time was up to 90 min. Adsorption experiments were carried out at 65, 75, 85 and 95 °C. Control experiments were used to check the degradation or adsorption of  $\beta$ -carotene and chlorophyll by the container walls in the absence of AAB. It was

**Table 2**  
Physical and chemical characteristics of the AAB sample.

Bulk density (g/ml)	Total pore volume (ml/g)	Specific surface area (m <sup>2</sup> /g)	Average pore diameter (nm)	Average particle size (μm)	Particle size distribution/wt. %			
					0–25.0 μm	25.0–38.5 μm	38.5–50.0 μm	50.0–74.0 μm
0.542	0.298	203.3	5.869	45.4	9.7	21.2	37.1	32.0

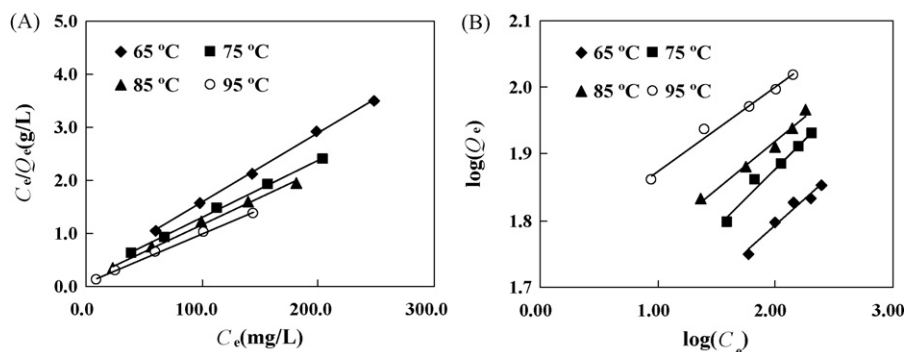


**Fig. 1.** The linearized adsorption isotherm of  $\beta$ -carotene in xylene solution onto AAB: (A) Langmuir isotherm, (B) Freundlich isotherm.

found that there was scarcely no degradation or adsorption of  $\beta$ -carotene and chlorophyll by container walls. All the experiments were performed in triplicate and the average values were used in calculation.

### 3. Results and discussion

#### 3.1. Equilibrium studies

The equilibrium data for adsorption of  $\beta$ -carotene and chlorophyll on AAB were analyzed using the Langmuir and Freundlich isotherms. The Langmuir adsorption Eq. (2), predicts the existence of monolayer coverage of the adsorbate at the outer surface of the adsorbent [24].

$$\frac{C_e}{Q_e} = \frac{1}{q_m K_L} + \frac{C_e}{q_m} \quad (2)$$

where  $C_e$  and  $Q_e$  are as defined in Eq. (1),  $q_m$  is the adsorption maximum (mg/g);  $K_L$  is the sorption equilibrium constant (L/mg). The Freundlich isotherm [24] is an empirical equation, which can be applied to heterogeneous systems, and is expressed by Eq. (3):

$$\log Q_e = \frac{1}{n} \log C_e + \log K_F \quad (3)$$

where  $K_F$  is a constant which reflects the adsorption capacity of the adsorbent for a specific solute, and  $n$  is a measure of the intensity of adsorption.

The plots of  $C_e/Q_e$  versus  $C_e$  for various  $\beta$ -carotene and chlorophyll initial concentrations were linear (Figs. 1 and 2). The constants  $q_m$  and  $K_L$ , can be calculated from the intercept and slope of the line, and are listed in Table 3. As seen from Table 3, the monolayer adsorption capacity  $q_m$  and  $K_L$  of  $\beta$ -carotene on the AAB increased with increasing temperature, and was maximum with 107.527 mg/g and 0.1574 L/mg at 95 °C, respectively. The higher value of  $K_L$  indicates a higher affinity for coloring material and more intense adsorption. The Langmuir model yielded a better fit than the Freundlich model of  $\beta$ -carotene adsorption with various temperatures, as reflected by correlation coefficients ( $R^2$ ) over 0.9950. Khoo et al. [13] reported similar observations about the suitability of Langmuir-type isotherm for the adsorption of  $\beta$ -carotene by

**Table 3**

Isotherm constants for adsorption of  $\beta$ -carotene and chlorophyll dissolved in xylene solution onto AAB.

Pigments	T (K)	Langmuir			Freundlich		
		$K_L$ (L/mg)	$q_m$ (mg/g)	$R^2$	$K_F$	$n$	$R^2$
$\beta$ -Carotene	338	0.0450	76.923	0.9993	29.964	6.329	0.9664
	348	0.0506	92.593	0.9989	33.427	5.653	0.9762
	358	0.0680	98.039	0.9950	42.678	6.897	0.9810
	368	0.1574	107.527	0.9983	55.899	7.918	0.9864
Chlorophyll	338	0.0724	9.728	0.9935	1.296	2.042	0.9980
	348	0.0876	10.081	0.9865	1.565	2.151	0.9962
	358	0.1423	10.152	0.9884	2.192	2.424	0.9968
	368	0.2644	10.173	0.9898	3.164	2.903	0.9951

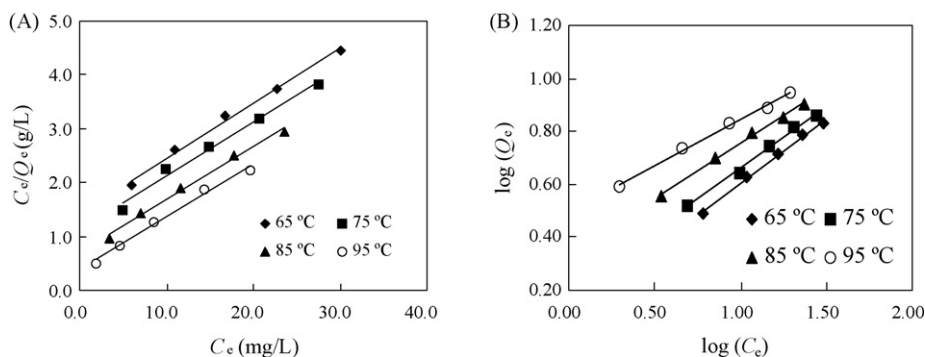


**Fig. 2.** The linearized adsorption isotherm of chlorophyll in xylene solution on AAB: (A) Langmuir isotherm, (B) Freundlich isotherm.

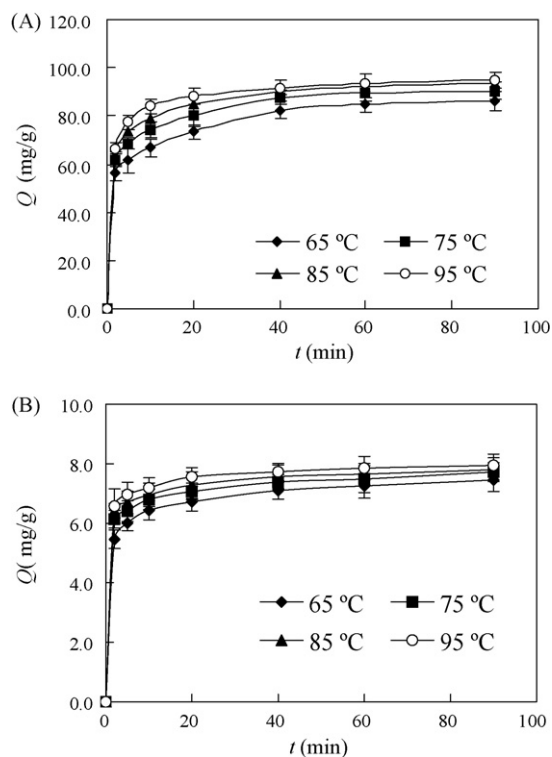


Fig. 3. Kinetic curves for adsorption of pigments dissolved in xylene solution on AAB at different temperatures: (A)  $\beta$ -carotene, (B) chlorophyll.

acid-activated montmorillonite. While in the parameters of the Freundlich equation, the value of  $n$  ranged between 0.1 and 1 indicated a favorable adsorption, and the larger  $K_F$  values at higher temperatures indicated more effective adsorption, and that the correlation coefficients ( $R^2$ ) from the Freundlich model was over 0.9664. So, the experimental data on  $\beta$ -carotene adsorption, at least extent, were fitted by the Freundlich isotherm. Surface heterogeneity could be caused by the existence of different acid centers on the smectite surface. Similarly, Christidis and Kosiari [12] reported that maize oil decolorization in the two steps showed indicative of a continuous coverage of the clay surface beyond a monolayer as indicated by Freundlich isotherms at equilibrium conditions, which attributed to the heterogeneity of smectite active centers and the existence of other active phases.

The Freundlich model fitted better than the Langmuir model with experimental data of chlorophyll adsorption at experimental temperatures, as reflected by correlation coefficients ( $R^2$ ) over 0.9951. In agreement with [17] who used acetone as solvent for chlorophyll-a. The observed increase in  $n$  and  $K_F$  with increasing temperature shows that higher temperature might cause more adsorption sites on AAB. While from the results shown in Fig. 3, experimental data of chlorophyll adsorption at experimental temperatures were also fitted by the Langmuir isotherm to a certain extent, as reflected by correlation coefficients ( $R^2$ ) over 0.9865.

### 3.2. Adsorption kinetics

Two kinetic models, pseudo-first-order and pseudo-second-order, were used to investigate the adsorption process of  $\beta$ -carotene and chlorophyll onto AAB, and to calculate the rate constants. The pseudo-first-order kinetic equation is expressed as [24]:

$$\log(Q_e - Q_t) = \log Q_e - \frac{k_1}{2.303} t \quad (4)$$

where  $k_1$  is the rate constant of pseudo-first-order sorption ( $\text{min}^{-1}$ ).

The pseudo-second-order kinetic equation is expressed as Eq. (5) [24]:

$$\frac{t}{Q_t} = \frac{1}{k_2 Q_e^2} + \frac{t}{Q_e} \quad (5)$$

where  $k_2$  is the rate constant of pseudo-second-order sorption ( $\text{g/mg min}$ ). The second-order rate constant can be determined from the intercept of the linearized pseudo-second-order equation.

The kinetic curves of  $\beta$ -carotene and chlorophyll adsorption at various temperatures are shown in Fig. 3. The equilibrium time of the  $\beta$ -carotene and chlorophyll adsorption from solution decreases with increasing temperatures. Hence higher temperature enhanced the adsorption rate. Temperature dependence is better expressed for  $\beta$ -carotene for which equilibrium attained after 40 min at 65 °C and after 20 min at 95 °C, while for chlorophyll adsorption, it rapidly attained equilibrium after 20 min for all experimental temperatures.

From the results shown in Fig. 3, the initial adsorption stage of pigments was very short in the first 10 min, followed by a gradual process till equilibrium was attained after a 60 min contact time, which indicated that the maximum sorption of pigments occurred after 1 h of bleaching. The adsorption process consisted of two distinguished periods, an initial period of rapid adsorption followed by a period of slow adsorption. The first fast step of adsorption could be due to the chemical interaction between  $\beta$ -carotene (or chlorophyll) and AAB surface, while the second slow step may indicate physical adsorption of pigments on those molecules diffused into pores of AAB following the first step. As previous studies [19] have shown the adsorption process of the two pigments on AAB was divided basically into two parts: a rapid adsorption stage which could be controlled by chemical interaction for initial 10 min, followed by a slow adsorption stage could be controlled by intraparticle diffusion till the attainment of equilibrium. Furthermore, the adsorption amount of  $\beta$ -carotene was clearly high as compared with that of chlorophyll under the same adsorption conditions. This may be attributed to the smaller molecular size and chain structure conformation,  $\beta$ -carotene molecules, with little space resistance, are easier to adsorb on the surface of AAB or diffuse into the pores of AAB, because their molecular size is  $2.1 \text{ nm} \times 0.8 \text{ nm} \times 0.7 \text{ nm}$  as compared to the larger molecular size of chlorophyll ( $3.0 \text{ nm} \times 1.7 \text{ nm} \times 1.3 \text{ nm}$ ) and net structure of chlorophyll [25].

The experimental data for the adsorption of the two pigments on AAB were fitted by the pseudo-first-order equation and pseudo-second-order equation, and values of  $k_1$ ,  $k_2$ ,  $Q_e$  and correlation coefficients are listed in Table 4. The correlation coefficient for the first-order kinetic model was lower and the theoretical  $Q_e$  values obtained from this model were not rational for the temperature range 65–95 °C. Hence the pseudo-first-order model did not commendably describe the adsorption results of  $\beta$ -carotene and chlorophyll onto AAB. The pseudo-second-order kinetic model of the both pigments yielded high correlation coefficient ( $R^2 > 0.9992$ ) at all experimental temperatures, and the theoretical  $Q_e$  values computed from this model were consistent with experimental  $q_{\text{exp}}$  values. However, the results obtained are considerably different from those of Khoo et al [13], who observed that adsorption of  $\beta$ -carotene from rapeseed oil has been found to follow a first-order rate law for low temperatures up to 35 °C. This is due to that  $\beta$ -carotene concentration in rapeseed oil is lower and the adsorption temperature is lower than our present studies. In addition, these results suggest that the adsorption process could involve a chemical interaction of valency forces by sharing of or proton exchange with proton between  $\beta$ -carotene (or chlorophyll) and AAB. Similarly, Christidis and Kosiari [12] and Sarier and Güler [14] have reported that adsorption of  $\beta$ -carotene on the activated clay was mainly a chemical process stemming from the interaction of  $\beta$ -

**Table 4**  
Kinetics constants for adsorption of  $\beta$ -carotene and chlorophyll dissolved in xylene solution onto AAB.

Pigments	T (K)	$q_{\text{exp}}$ (mg/g)	Pseudo-first-order kinetic model			Pseudo-second-order kinetic model		
			$k_1$ (min <sup>-1</sup> )	$Q_e$ (mg/g)	$R^2$	$k_2$ (g/mg min)	$Q_e$ (mg/g)	$R^2$
$\beta$ -Carotene	338	88.355	0.0320	29.221	0.9690	0.0043	88.496	0.9992
	348	92.017	0.0341	25.154	0.9556	0.0054	92.593	0.9996
	358	93.611	0.0491	26.424	0.9899	0.0063	94.340	0.9997
	368	94.957	0.0470	21.662	0.9833	0.0078	96.154	0.9999
Chlorophyll	338	7.756	0.0214	1.839	0.9522	0.0808	7.525	0.9995
	348	7.954	0.0212	1.596	0.9646	0.0941	7.758	0.9995
	358	8.045	0.0189	1.337	0.9132	0.1154	7.849	0.9997
	368	8.109	0.0223	1.269	0.9409	0.1267	8.019	0.9998

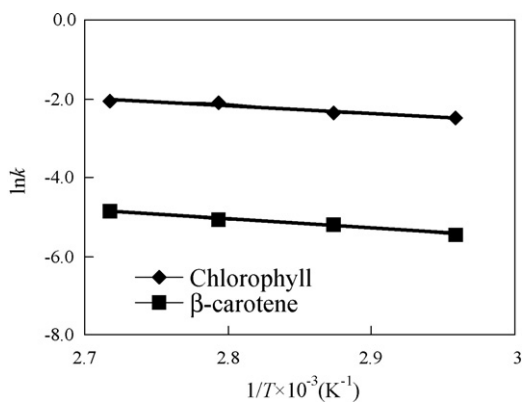


**Fig. 4.** Arrhenius plots for adsorption of the two pigments onto AAB at different temperatures.

carotene with the Lewis and Brønsted acid sites of clay from the differential thermal analysis and the infrared spectroscopy of the acid-activated montmorillonite with adsorbed  $\beta$ -carotene. Similarly, the chlorophyll molecules are mainly adsorbed on Brønsted acid sites and held electrostatically on the AAB surface [15,16].

### 3.3. Thermodynamics parameters

The activation energy,  $E_a$  of a reaction, is obtained from an Arrhenius equation (6) [12]:

$$\ln(k) = \ln(A) - \frac{E_a}{R} \left( \frac{1}{T} \right) \quad (6)$$

where  $A$  the frequency factor or the Arrhenius constant,  $R$  the universal gas constant (8.314 J/K mol),  $T$  the absolute temperature, and  $k$  the rate constant; in this case  $k$  is given by the pseudo-second-order rate constant  $k_2$ .

When  $\ln k$  is plotted against the reciprocal of the temperature ( $1/T$ ), as in Fig. 4,  $E_a$  represents the slope is shown in Table 5. The activation energy for the sorption of  $\beta$ -carotene and chlorophyll on AAB was estimated as 19.808 kJ/mol and 16.475 kJ/mol, respectively. These values of activation energy  $E_a$  are mainly characteristic

physical adsorption mechanisms. And the whole adsorption process could be finally controlled by physical adsorption (diffusion).

The data obtained from adsorption isotherm models can be conveniently used to determine, such thermodynamic parameters as free energy of adsorption  $\Delta G^\theta$ , enthalpy change of adsorption  $\Delta H^\theta$  and the change in standard entropy  $\Delta S^\theta$ . These parameters are evaluated using the following equation:

$$K_d = K_F = X \quad (7)$$

where  $K_d$  (L/mol) is the sorption distribution coefficient. The  $K_d$  values were plugged into Eq. (7) to determine the free energy of sorption process at various temperatures [26].

$$\Delta G^\theta = -RT \ln K_F \quad (8)$$

where  $\Delta G^\theta$  is the free energy of sorption (kJ/mol). Enthalpy change  $\Delta H^\theta$  and entropy change  $\Delta S^\theta$  values were calculated at different temperatures by the following (Eq. (8)) [26]:

$$\ln K_F = -\frac{\Delta H^\theta}{RT} + \frac{\Delta S^\theta}{R} \quad (9)$$

where  $K_F$  is the adsorption equilibrium constant in Eq. (3) for the two pigment adsorptions.

When  $\ln K_F$  against the temperature ( $1/T$ ) is plotted, as in Fig. 5, the results of the thermodynamic parameters have been evaluated for the sorption system of  $\beta$ -carotene and chlorophyll at 65, 75, 85 and 95 °C, and represented in Table 5. The negative value of  $\Delta G^\theta$  indicates the spontaneous of  $\beta$ -carotene and chlorophyll adsorption on AAB. The values of  $\Delta G^\theta$  increased lightly with increasing the temperature, indicating the affinity between  $\beta$ -carotene (or chlorophyll) and AAB surface enhanced with increasing the temperature. This shows that the removal process is favored at higher temperature. The positive value of  $\Delta H^\theta$  indicated that the adsorption process was an endothermic one, which was in agreement with what described above, namely the amount of  $\beta$ -carotene and chlorophyll is increased with increasing the temperature. Obviously, the adsorption of the two pigments on AAB was entropically driven. The positive values of  $\Delta S^\theta$  suggest increased randomness at the solid–solution interface during the two pigment adsorption processes.

**Table 5**  
Thermodynamic parameters for adsorption of ( $\beta$ -carotene and chlorophyll dissolved in xylene solution onto AAB.

Pigments	T (K)	$k_2$ (g/mg min)	$E_a$ (kJ/mol)	$K_F$	$\Delta H^\theta$ (kJ/mol)	$\Delta S^\theta$ (J/K mol)	$\Delta G^\theta$ (kJ/mol)
$\beta$ -Carotene	338	0.0043	19.808	29.964	21.766	92.244	-9.554
	348	0.0054		33.427	21.766	92.244	-10.153
	358	0.0063		42.678	21.766	92.244	-11.172
	368	0.0078		55.898	21.766	92.244	-12.310
Chlorophyll	338	0.0808	16.475	1.296	31.051	93.549	-0.729
	348	0.0941		1.565	31.051	93.549	-1.296
	358	0.1194		2.192	31.051	93.549	-2.336
	368	0.1267		3.165	31.051	93.549	-3.525

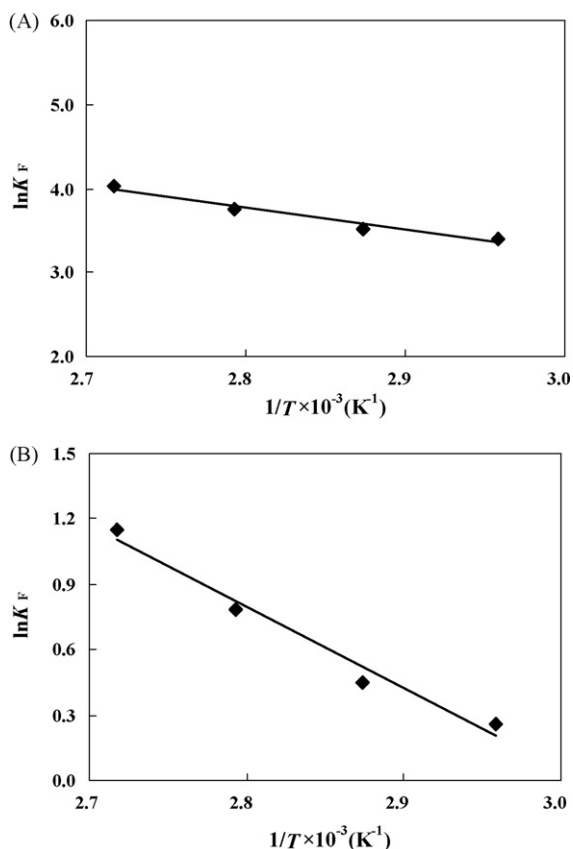


Fig. 5.  $\ln K_F$  vs.  $1/T$  plots for adsorption of the two pigments onto AAB at different temperatures: (A)  $\beta$ -carotene, (B) chlorophyll.

#### 4. Conclusions

The use of an AAB from Xinjiang in China as adsorbent of  $\beta$ -carotene and chlorophyll from xylene solution at temperatures 65–95 °C has been examined.  $\beta$ -Carotene adsorption was described well by the Langmuir model, whereas the Freundlich model fitted better with experimental data on chlorophyll adsorption. Higher temperature was favor of enhancing the adsorption of  $\beta$ -carotene and chlorophyll on AAB. The kinetics results indicated that the adsorption of  $\beta$ -carotene and chlorophyll was described by the pseudo-second-order equation  $\beta$ -carotene and chlorophyll, and suggested that the adsorption involved chemical interaction. The activation energy values indicated that the overall adsorption process of  $\beta$ -carotene and chlorophyll was physical adsorption. The sorption of  $\beta$ -carotene and chlorophyll onto AAB was spontaneous, endothermic, and entropically driven. The randomness increased at the solid–solution interface during the two pigment adsorption processes.

#### Acknowledgements

This work was financially supported by the Ministry of Education “Chunhui Plan” International Cooperation Project

(Z2006-1-83018), Xinjiang Bingtuan Key Science and Technology Industry Project (2008GG24) and Shihezi University’ High Level Talent Start Fund Project (RCZX200636) P. R. China.

#### References

- [1] E.Y. Park, H. Ming, Oxidation of rapeseed oil in waste activated bleaching earth and its effect on riboflavin production in culture of *Ashbya gossypii*, J. Biosci. Bioeng. 97 (2004) 59–64.
- [2] D. Siguín, S. Ferreira, L. Foufre, F. García, Smectites: the relationship between their properties and isomorphic substitution, J. Mater. Sci. 29 (1994) 4379–4384.
- [3] X.F. Sun, C. Li, Z.S. Wu, X.L. Xu, L. Ren, H.S. Zhao, Adsorption of protein from model wine solution by different bentonites, Chin. J. Chem. Eng. 15 (2007) 632–638.
- [4] P. Kumar, R.V. Jasra, T.S.G. Bhat, Evolution of porosity and surface acidity in montmorillonite clay on acid activation, Ind. Eng. Chem. Res. 34 (1995) 1440–1448.
- [5] S.R. Chitnis, M.M. Sharma, Industrial applications of acid-treated clays as catalysts, React. Funct. Polym. 32 (1997) 93–115.
- [6] E. Srasra, F. Bergaya, H.V. Damme, N.K. Ariguib, Surface properties of an activated bentonite decolorisation of rape-seed oils, Appl. Clay Sci. 4 (1989) 411–421.
- [7] S.C. Kheok, E.E. Lim, Mechanism of palm oil bleaching by montmorillonite clay activated at various acid concentrations, J. Am. Oil Chem. Soc. 59 (1982) 129–131.
- [8] K.S. Low, K.C. Lee, L.Y. Kong, Decolorisation of crude palm oil by acid-activated spent bleaching earth, J. Chem. Technol. Biotechnol. 72 (1998) 67–73.
- [9] W.P. Gates, J.S. Anderson, M.D. Raven, G.J. Churchman, Mineralogy of a bentonite from Miles, Queensland, Australia and characterization of its acid activation products, Appl. Clay Sci. 20 (2002) 189–197.
- [10] P. Falaras, I. Kovanis, F. Lezou, G. Seiragakis, Cottonseed oil bleaching by acid-activated montmorillonite, Clay Miner. 34 (1999) 221–232.
- [11] M. Rossi, M. Gianazza, C. Alamprese, F. Stanga, The effect of bleaching and physical refining on colour and minor components of palm oil, J. Am. Oil Chem. Soc. 78 (2001) 1051–1055.
- [12] G.E. Christidis, S. Kosiari, Decolorization of vegetable oil: a study of the mechanism of adsorption of  $\beta$ -carotene by an acid-activated bentonite from Cyprus, Clays Clay Miner. 51 (2003) 327–333.
- [13] L.E. Khoo, F. Moorsingh, K.Y. Liew, The adsorption  $\beta$ -carotene by bleaching earths, J. Am. Oil Chem. Soc. 56 (1979) 672–675.
- [14] N. Sarier, C. Güler, The mechanism of  $\beta$ -carotene adsorption on acid-activated montmorillonite, J. Am. Oil Chem. Soc. 66 (1989) 917–923.
- [15] G. Güler, F. Tunc, Chlorophyll adsorption on acid-activated clay, J. Am. Oil Chem. Soc. 69 (1992) 948–950.
- [16] R. Mokaya, W. Jones, M.E. Davies, M.E. Whittle, The mechanism of chlorophyll adsorption on acid-activated clays, J. Solid State Chem. 111 (1994) 157–165.
- [17] E.G. Pradas, M.V. Sánchez, M.S. Viciano, A.G. Campo, Adsorption of chlorophyll-a from acetone solution on natural and activated bentonite, J. Chem. Technol. Biotechnol. 61 (1994) 175–178.
- [18] Z.S. Wu, C. Li, X.F. Sun, X.L. Xu, B. Dai, J.E. Li, H.S. Zhao, Characterization, acid activation and bleaching performance of bentonite from Xinjiang, Chin. J. Chem. Eng. 14 (2006) 253–258.
- [19] J.M. Tong, Z.S. Wu, X.F. Sun, X.L. Xu, C. Li, Adsorption kinetics of  $\beta$ -carotene and chlorophyll from model oil solutions onto acid activated bentonite, Chin. J. Chem. Eng. 16 (2008) 270–276.
- [20] Writers Group of Mineral Analyses of Rocks, Mineral Analyses of Rocks, third ed., Geology Press, Beijing, 1991, pp. 1060–1075 (in Chinese).
- [21] Y. Bai, Z.S. Mu, G.X. Zhang, Extraction technology of  $\beta$ -carotene, Inner Mongolia Agric. Sci. Technol. 4 (2002) 12–13.
- [22] Y.S. Peng, E. Liu, Studies of method on extract chlorophyll a and b, Catal. Agric. Univ. Pekinensis 18 (1992) 247–250.
- [23] G.M. Duan, Derivation of Arnon formula on determination of chlorophyll content, Plant Physiol. Commun. 28 (1992) 221–222.
- [24] A.Y. Dursun, C.S. Kalayci, Equilibrium, kinetic and thermodynamic studies on the adsorption of phenol onto chitin, J. Hazard. Mater. B123 (2005) 151–157.
- [25] J.H. Huang, Y.F. Liu, Y. Liu, X.G. Wang, Effect of attapulgite pore size distribution on soybean oil bleaching, J. Am. Oil Chem. Soc. 84 (2007) 687–692.
- [26] E. Sabah, M. Cinar, M.S. Celik, Decolorization of vegetable oils: adsorption mechanism of  $\beta$ -carotene on acid-activated sepiolite, Food Chem. 100 (2007) 1661–1668.